Direct Measurement of the Cohesive Law of Adhesives Using a Rigid Double Cantilever Beam Technique

A. Khayer Dastjerdi · E. Tan · F. Barthelat

Abstract Engineering adhesive joints are being increasingly used in industry because of the advantages they offer over other joining methods such as fastening or welding. The development and the use of adhesives in a design environment require accurate mechanical tests in order to measure their strength and toughness. Standard techniques such as the shear lap test are commonly used to measure shear strength, but the results they produce generally depend on geometry and on initial defects within the bond line. Fracture tests such as the double cantilever beam (DCB) tests overcome these limitations, but rely on elasticity models and assumptions to determine toughness. In this study, we present a novel technique to directly determine the mode I fracture toughness of engineering adhesive joints as well as their full cohesive law, without any initial assumption on its shape. Our new method is remarkably simple in terms of experimental setup, execution and analysis. It is similar to the standard double cantilever beam (DCB) test with the difference that the material and dimensions of the beams are chosen so that they are assumed to be rigid compared to the bond line. In this rigid DCB (RDCB) technique the crack opening is known everywhere along the interface, which we use to compute the cohesive law of the adhesive directly from the load-displacement data obtained from experiment and the geometry of the RDCB specimen. The RDCB method is validated and applied to three typical commercial adhesives (polyurethane, epoxy, and silicone), to determine their cohesive law and fracture toughness.

Keywords Cohesive law · Fracture toughness · Double cantilever beam · Adhesives

A. Khayer Dastjerdi · E. Tan · F. Barthelat (✉)
Department of Mechanical Engineering, McGill University,
817 Sherbrooke Street West,
Montreal, QC, Canada H3A 2K6
e-mail: francois.barthelat@mcgill.ca

Introduction

Engineering adhesives are been increasingly used in various industries such as automotive and aerospace for bonding various structures [1, 2]. Adhesive joints provide several advantages over classical joining methods such as fastening or spot welding. Glued components transfer stresses more uniformly even if they are made of dissimilar materials, and a glued joint is lighter and less expensive than other traditional joining methods [1]. The shear lap test is a widely used test method to characterize the performance of adhesive-bonded joints subjected to shear loading [3]. Despite the fact that the strength of an adhesive interface is a key factor controlling its mechanical performance, it is now well-understood that the strength of a material is affected by presence of defects and flaws which may form due to inaccurate joint assembly or inappropriate curing. Under certain loading condition, these flaws may propagate into large cracks and lead to the failure of the material. It is therefore essential to characterize and evaluate the toughness of the bond line, which directly affects strength, reliability and energy absorption of the material. There are several experimental techniques which can be used to measure the fracture toughness of adhesive joints under mode I fracture loading (opening mode). These include double cantilever beam (DCB) test [4, 5], blister test [6], and indentation test [7, 8]. Amongst these techniques the DCB test has gained the most popularity because of its relative simplicity, and it has been adopted as an ASTM standard [9]. A DCB specimen consists of two beams of uniform thickness, bonded together by a thin layer of adhesive only partially covering the length of the beams. The specimen is loaded by pulling the free ends of the two beams in a direction normal to the fracture surface, so that a crack extends along the interface of the two beams. The elastic energy is stored in the deformed portion of the beams (which have the configuration of two cantilever beams) and it is released upon

crack extension. The energy released is then used to measure the toughness (energy required to extend a crack) of the adhesive [4, 10]. The basic DCB technique can be augmented by for example *in-situ* imaging, which enables the determination of the cohesive law (traction-separation function) of the adhesive [11–16]. The cohesive law of the adhesive can then serve as the basis for cohesive zone modeling (CZM), which is a powerful technique to simulate crack initiation and growth often used to model fracture and fragmentation processes in metallic, polymeric, and ceramic materials and their composites [17–19]. In order to propagate the crack by an increment of distance, the cohesive forces will produce work over the opening distance, so that the toughness (in terms of energy per unit surface) is simply obtained by measuring the area under the cohesive law. If cracking has reached a steady state, the fracture behavior does not depend on the shape of the cohesive law [20]. However, in non-steady regimes or dynamic loading situations, details of the cohesive law are needed to properly capture and predict crack propagation. The full cohesive law provides more information (including the maximum traction exerted by adhesive on the crack walls, stiffness of the adhesive layer, and maximum separation prior to the final de-cohesion) than a single toughness value, which makes it more valuable in the context of the design and optimization of novel adhesive compounds. The experimental determination of the full cohesive law is more involving than measuring toughness, and the available methods can be classified into two main categories: direct and inverse techniques. In direct methods, the cohesive law is determined directly from fracture experiments [11–13, 21–24] using for example J-integral contours. These techniques can be difficult and are rather involved in terms of experimental capabilities. For instance, Biel et al. [13] determined the cohesive law of an adhesive layer using DCB technique, with two LVDTs to measure the separation of the adhesive layer at the crack tip and an incremental shaft encoder to measure the rotation at the tip of the DCB beams. The inverse methods represent another type of approach which consists in modeling the experiment using finite elements, and identifying the parameters of the cohesive law which produce the best match between the model and the experiments [11, 25–27]. While the experimental setup can be quite simple, the analysis relies on the accuracy of numerical models, and may suffer from problems associated with non-uniqueness of the solution. In general, direct and indirect methods assume a shape for the cohesive law, typically a bi-linear function (triangular cohesive law), which is characterized by three independent parameters (for example strength, maximum opening and toughness). In spite of the usefulness of these techniques, a streamlined method to directly measure cohesive laws without experimental and numerical complications is needed. In this article, we present a novel and simple

experimental approach to measure the cohesive law of engineering adhesives. We first developed this technique to measure the interfacial fracture toughness of soft biological adhesives such as fibrin clot in blood coagulation [5]. Because of the simplicity and high potential of the technique we have now modified it to measure the cohesive law of engineering adhesives. The new rigid-double-cantilever-beam (RDCB) technique is similar in concept to the standard DCB test, with an important difference: the substrates are assumed to be rigid. In the RDCB configuration the strain energy eventually released upon crack propagation is therefore stored in the adhesive itself, as opposed to the traditional DCB setup where the strain energy is predominantly stored in the deflected beams. The assumption of rigid substrates also means that the opening of the adhesive can be easily computed along the entire bond line, without the need for contact or non-contact optical extensometers. The analysis for this test is also extremely simple, and directly leads to the full cohesive law of the adhesive, without any initial assumption on its shape.

Experimental Setup

The setup for our new rigid double cantilever beam (RDCB) experiment is similar to the traditional DCB, but the substrates are designed to be sufficiently stiff to be assumed rigid with respect to the adhesive. Here two thick steel blocks were used as substrates as shown in Fig. 1(a). The adherent surface was mirror polished down to 0.05 μm particle size in order to ensure a smooth surface, minimizing the effect of roughness on the results. Rougher surfaces were not considered in this work, although they can easily be implemented in the experimental protocol. The adhesive was used to join the two blocks, by partially covering their interfaces. The sample was then mounted on a miniature loading stage (Ernest F. Fullam, Inc, Latham, NY) operated horizontally (Fig. 1(b)). Two steel pins symmetrically located at the both sides of the center line were used to apply displacement at a rate of 50 μm/s, through slots machined in the RDCB sample, thereby opening the adhesive layer in mode I (Fig. 1(b)).

The force and displacement were measured during the experiment using a 100 lbs load cell and a LVDT. Machine compliance was measured by mounting a calibration sample consisting of a single steel block with the same overall dimensions and the same slot as shown on Fig. 1(a), but with no interface (i.e. the calibration sample resembles the RDCB blocks with their interface "fused"). The compliance of the machine was $C_m=1 \mu m/N$. We corrected the total displacement Δ_{total} obtained from experiment to obtain the opening of the RDCB specimen Δ using $\Delta = \Delta_{total} - C_m F$ where F is the force.
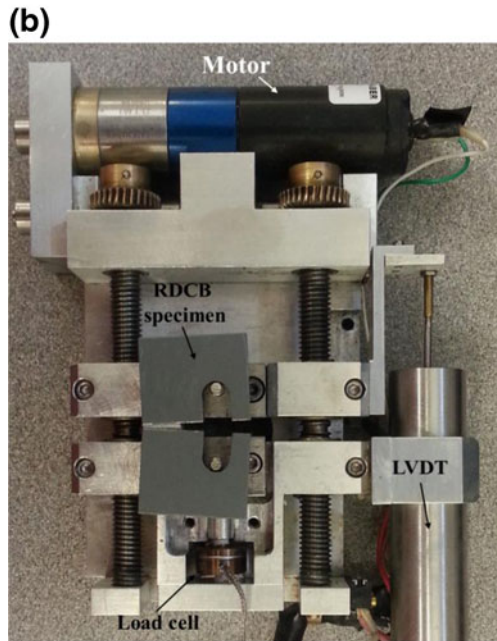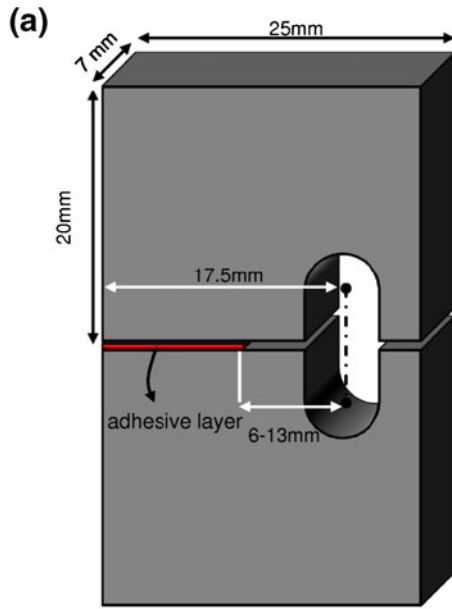
failing it in mode I fracture. The assumption of rigid substrates enables a simple and direct calculation of the opening of the interface anywhere along the bond line:

$$u(x) = \frac{x}{L}\,\Delta \tag{1}$$

Where Δ is the pin separation displacement (as measured from the LVDT corrected for machine compliance), L is the distance from point O to the line of action of the pulling force and x is the position from point O. With equation (1) the opening is known along the entire bond line, which enables the determination of the full cohesive law for the interface.

Balancing the moment exerted by the closure force of the adhesive with the moment generated by the applied force F (about point O) gives:

$$B\int_0^b xt(x)dx = LF \tag{2}$$

Where B is the width of the beams, b is the length of the bond line, and L is the distance from point O to the line of action of the pulling force. $t(x)$ denotes the traction function. Since the opening is known along the entire length of the substrate, equation (1) can be used for a change of variable in equation (2), giving:

$$\left(\frac{L}{\Delta}\right)^2 \int_0^\delta ut(u)du = \frac{L}{B}\,F \tag{3}$$

Fig. 1 (a) Schematic illustration of the RDCB sample geometry; (b) actual picture of the setup showing an opened sample mounted on the miniature loading stage

Data Analysis: Measuring Cohesive Laws

The RDCB analysis relies on the assumption that the substrates are rigid compared to the adhesive bond line, and the validity of this assumption is discussed in detailed in "Validity of the Substrate Rigidity Assumption" section below. If the substrate is assumed to be rigid, the system is greatly simplified (Fig. 2). Upon opening of the interface the two blocks simply rotate about a hinge point (point O in Fig. 2), thereby stretching the bond line and eventually
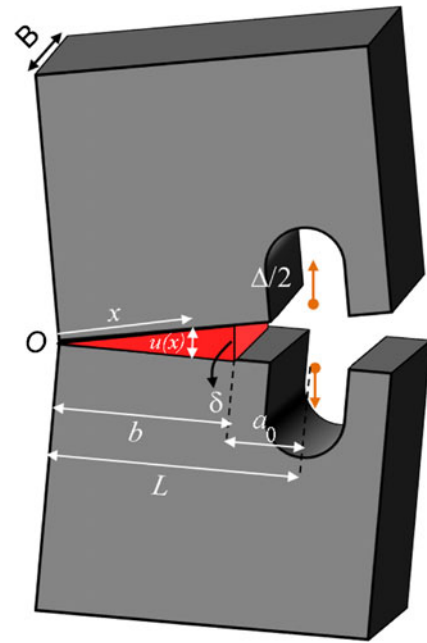
Where δ denotes separation at the crack tip. This equation is then differentiated with respect to δ, leading to:

$$\delta t(\delta) = \frac{d\,\Delta}{d\,\delta}\frac{d}{d\,\Delta}\left(\frac{\Delta^2}{BL}F\right) \tag{4}$$

Using $\delta = \frac{b}{L}\Delta$ leads to an expression for the cohesive law of the interface:

$$t(\delta) = \left(\frac{L}{B(L-a_0)^2}\right)\left(2F + \Delta\frac{dF}{d\,\Delta}\right) \tag{5}$$

Where a_0 is the initial crack length (Fig. 2). The cohesive law of the interface can therefore be easily obtained from the load-displacement curve and its derivative, and from the geometry of the specimen. Equation (5) does not require any initial assumption on the shape of the cohesive law, which is a significant advantage. Once the cohesive law is computed, the toughness of the interface is then simply given by the area under the cohesive law:

$$J_{IC} = \int_0^\infty t(u)\,du \tag{6}$$

The toughness obtained from equation (6) is equal to the work-of-fracture, defined as the area under the $(F\text{-}\Delta)$ divided by the initial surface area of the adhesive (i.e. work-of-fracture measures the energy required to separate a unit surface of adhesive). Since the traction function becomes zero at separations larger than the maximum separation (δ_{max}), it does not make any difference if the upper limit of the integral is infinity or δ_{max}. In order to validate the RDCB test we tested a 1 mm-thick double-sided polyethylene foam adhesive tape, producing the load-deflection curve shown in Fig. 3(a). The force increased with opening, until a maximum of 4 N at the onset of crack propagation. Thereafter the force progressively decreases until almost complete separation of the two substrates at an opening of 8 mm. Equation (5) was then used to compute the full cohesive law of the adhesive tape, with the results shown on Fig. 3(b). The initial region of the cohesive laws is linear which corresponds to the elastic deformation of the interface. At a separation of ~300 µm, the interface starts softening, which could correspond to nonlinear response of the adhesive or to the onset of cavitation in the adhesive. The damage accumulation continues until the cohesive law reaches a maximum (i.e. cohesive strength which is ~180 kPa) after which the interface progressively softens as damage increases. Once the adhesive opening reaches the maximum separation (~1,200 µm), the cohesive traction at the interface vanishes, corresponding to full decohesion. The toughness of the adhesive layer is then simply given by the area under the
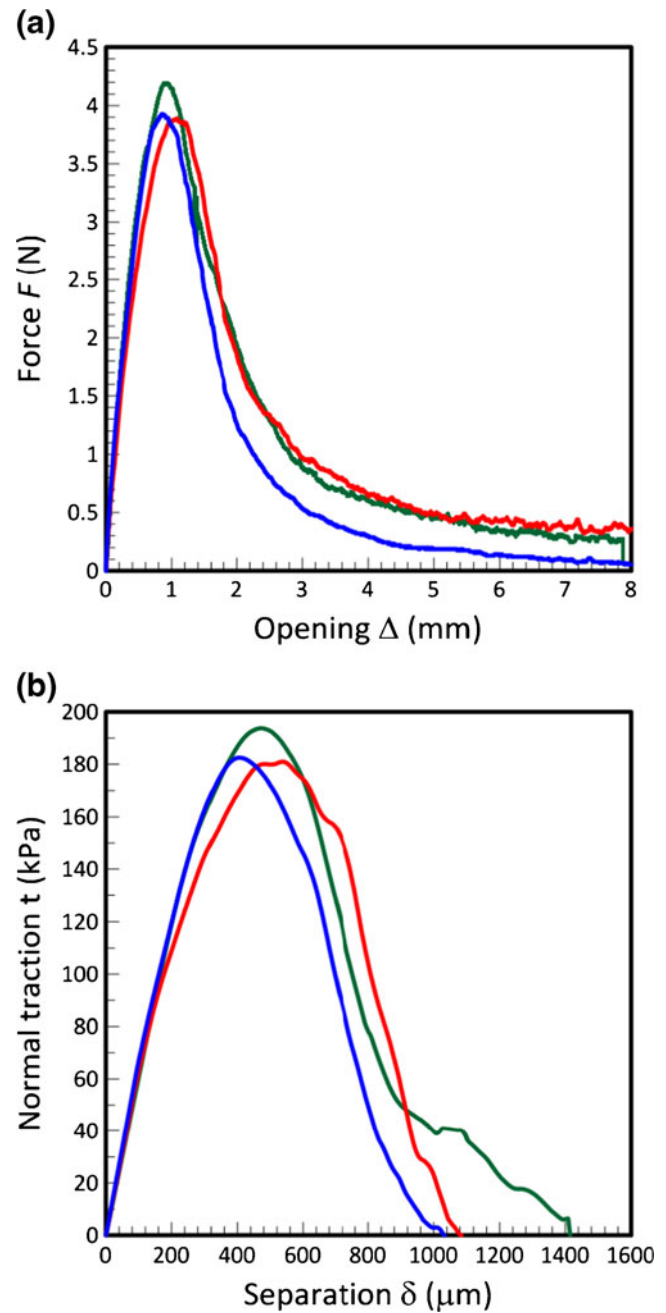

Fig. 3 (a) Typical force-displacement curves for double-sided polyethylene foam adhesive tape; (b) corresponding cohesive laws determined from the RDCB model

cohesive law, in this case $J_{IC}=116\pm21$ J/m^2 (five specimens were tested). For validation we also measured the toughness of this adhesive (taped on the same polished steel surface) using a standard peel test configuration (ASTM D6862-04) which gave a toughness of $J_{IC}=127\pm15$ J/m^2 (five specimens were tested). The values given by the RDCB and peel tests are comparable within experimental errors, which validated the RDCB test procedure and data analysis.

Validity of the Substrate Rigidity Assumption

The RDCB analysis relies on the assumption of a rigid substrate compared to the adhesive. For this assumption to be valid, the deformations of the substrate should be negligible compared to the deformation of the adhesive. These deformations depend on the force carried through the system, and during the RDCB test the force is at the highest at the end of the elastic regime for the adhesive. Past the yield point of the adhesive the force decreases and the substrates unload. Consequently, it is at the yield point of the adhesive that the deflection of the substrates is the largest. In order to examine the validity of the RDCB assumption, it is therefore sufficient to compare the deflections of the substrates and adhesives in the elastic regime.

In order to identify the critical parameters governing the deflections of the substrate and the adhesive layer, the free body diagram in Fig. 4 was considered. The opening force was modeled as point load, and the adhesive was modeled as a linear distribution of tractions, consistent with a linear elastic regime. By balancing the external work done by load P and moment $P(L - b)$ with the energy stored within the half thickness of the adhesive layer, we obtain:

$$P\delta_{tip} + P(L-b)\frac{\delta_{tip}}{b} = 1\Big/2 \int_0^b SBu^2 dx \qquad (7)$$

Where u is opening at distance x from the hinge point O, δ_{tip} is half the crack tip separation (at $x = b$) when traction reaches the cohesive strength of the interface σ_m, S is the stiffness of the half thickness of the adhesive layer. Since we consider half the adhesive thickness, the separation is divided by two (while the traction does not change), therefore $S = \frac{t}{\delta/2} = 2S_{int}$,
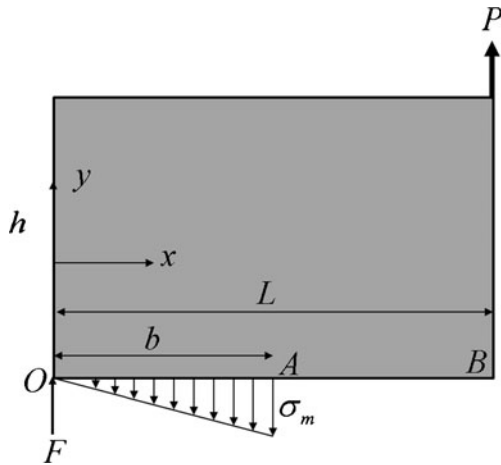

Fig. 4 Free body diagram of the upper section of the substrate in RDCB configuration

where S_{int} is the initial slope of the cohesive law. Using $u = \frac{\delta_{tip}}{b}x$, equation (7) yields:

$$\delta_{tip} = \frac{3PL}{Bb^2 S_{int}} \qquad (8)$$

The maximum deflection of the substrate occurs when the traction at the crack tip reaches the cohesive strength of the interface σ_m. At this point the defection of the substrate can be obtained using Castigliano's second theorem [28], considering deformations from bending moments and from shear forces. The substrate is also divided into two sections $0<x<b$ and $b<x<L$. The strain energy of the system can then be written as:

$$U = \int_0^b \frac{M_1^2}{2EI}dx + \int_0^b \frac{3V_1^2}{5GA}dx + \int_b^L \frac{M_2^2}{2EI}dx + \int_b^L \frac{3V_2^2}{5GA}dx \qquad (9)$$

where M_i and V_i are bending moment and shear load, respectively, G and E are shear modulus and Young's modulus of the substrate, respectively. A, I, and L denote the substrate cross section area, the substrate second moment of area, and the distance from loading line to the hinge point O, respectively. Writing force equilibrium in y direction and moment equilibrium around point O gives $F = \left(\frac{3L}{2b}-1\right)P$ and $\sigma_m = \frac{3PL}{Bb^2}$. The bending moment and shear load in $OA(M_1$ and $V_1)$ and AB $(M_2$ and $V_2)$ part of the substrate can be written:

$$\begin{cases} M_1 = \dfrac{B\sigma_m x^3}{6b} + \left(1-\dfrac{3L}{2b}\right)Px \\ V_1 = -\dfrac{\sigma_m B}{2b}x^2 - \left(1-\dfrac{3L}{2b}\right)P \\ M_2 = P(L-x) \\ V_2 = P \end{cases} \qquad (10)$$

Substituting for shear loads and bending moments from equation (10) into equation (9), and taking derivative from equation (9) with respect to P yields the deformation of the substrate at the loading line:

$$\delta_1 = P\left(\frac{\alpha_s}{GA} + \frac{\alpha_b}{EI}\right) \qquad (11)$$

With

$$\begin{cases} \alpha_s = \dfrac{9}{5}L\left(\dfrac{L}{b}-1\right) \\ \alpha_b = \left(\dfrac{L^3}{3} + \dfrac{Lb^2}{10} - \dfrac{2L^2b}{5}\right) \end{cases} \qquad (12)$$

Equation (11) can further be simplified with assuming a homogeneous isotropic linear elastic property for the substrate material (with rectangular cross section):

$$\delta_1 = \frac{P\big((1+v)\alpha_s' + \alpha_b'\big)}{E} \quad (13)$$

With

$$\begin{cases} \alpha_s' = \dfrac{2\alpha_s}{Bh} \\[2mm] \alpha_b' = \dfrac{12\alpha_b}{Bh^3} \end{cases} \quad (14)$$

Where v and h are the poison's ratio and thickness of the substrate, respectively. In addition to this opening, resulting from bending moments and from shear forces, the adhesive layer separation also produces opening along the loading line which must be considered in the calculations. This is taken into account by rotating the substrate around the hinge point O so that the crack tip opens up to $2\delta_{tip}$ which gives:

$$\delta_2 = \left(\frac{L}{b}\right)\delta_{tip} \quad (15)$$

Then the total substrate tip opening is obtained through adding opening from (13) to (15):

$$\Delta = P\left(\frac{(1+v)\alpha_s' + \alpha_b'}{E} + \frac{3L^2}{Bb^3 S_{int}}\right) \quad (16)$$

We now define the nondimensional ratio $\alpha = \frac{\delta_{tip}L}{\Delta b}$ which can be used as a parameter to assess the rigidity of the substrate. This ratio must be equal, or close to unity for the substrate to be considered rigid. In this case the surface of the substrate remains uniformly straight and equation (1) can be used. Substituting half the crack tip opening from (8) and the substrate tip opening from (16) into this ratio results:

$$\alpha = \frac{\delta_{tip}L}{\Delta b} = \left(1 + \frac{Bb^3 S_{int}\big((1+v)\alpha_s' + \alpha_b'\big)}{3L^2 E}\right)^{-1} \quad (17)$$

Equation (17) can now be used to assess the validity of the rigid substrate assumption. It incorporates the geometry of the specimens, as well as the elastic properties of the substrate and the cohesive strength of the adhesive layer. The equation is illustrated on Fig. 5, which shows the ratio α as a function of dimensionless material parameter $\frac{\sigma_m}{E}$ (ratio of the cohesive strength of the interface to the modulus of the substrate) for the fixed dimensions specified in Fig. 1. The model confirms that the ratio is equal to one for low cohesive strength of the adhesive and/or high substrate modulus. When the ratio $\frac{\sigma_m}{E}$ gets larger, α deviates from unity, indicating substrate deformation. α becomes smaller than 0.95 for $\frac{\sigma_m}{E} > 8.3 \cdot 10^{-4}$. As the ratio α becomes larger the traditional DCB method becomes more appropriate.

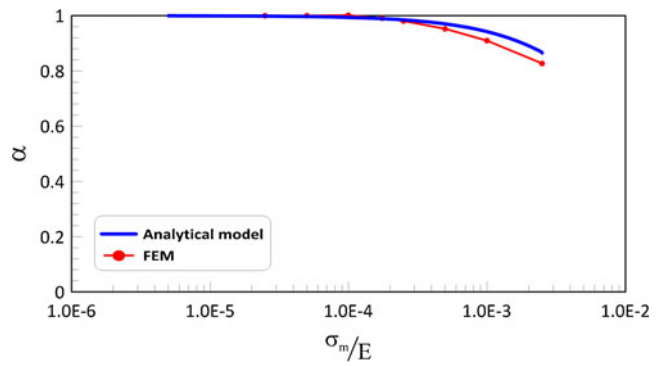**Fig. 5** α as a function of dimensionless parameter $\frac{\sigma_m}{E}$ showing intimate agreement between results obtained from finite element and from analytical model (equation (17))

The effect of substrate geometry on its rigidity can also be easily assessed using equation (17). Figure 6 shows the effect of geometry for a fixed ratio $\frac{\sigma_m}{E} = 2.5 \cdot 10^{-4}$. As expected short and thick beams lead to α close to unity, and this ratio decreases for more slender beams.

Finally, we verified equation (17) using finite element method. The RDCB configuration was constructed in ABAQUS (v. 6.9, ABAQUS Inc., Providence, RI), with the geometry shown in Fig. 1. Using symmetry about the plane defined by the bond line, only the upper half of the system was modeled: one substrate, and half of the thickness of the bond line. The substrate was modeled as linear elastic with plane strain condition. The interface was modeled using zero thickness interface elements in which the cohesive law is embedded through a user-defined Fortran subroutine. The material properties of the interface are therefore not needed; the upper nodes joined with the nodes from the substrate, and the lower nodes only constrained to remain on the plane of symmetry. A trapezoidal cohesive law was chosen to simulate crack propagation within the adhesive layer. Since the main concern of this work is measuring the substrate deformation at the onset of interface softening, we only considered the results at the end of the linear part of the cohesive law. Hence the way at which the interface softens does not play any role in the results. The upper pin of the fixture was modeled as a rigid surface in contact with the inner surface of the fixture. The pin was displaced at a fixed rate to simulate the opening of the interface. Figure 5 shows a good agreement between the finite element results and the analytical result of equation (17).

Example of RDCB Tests on Three Typical Engineering Adhesives

The adhesives we explored in this work covered a wide range of mechanical behavior from soft elastomers to stiff thermoset polymers: silicone (Silicone, General Electric, Huntersville, NC, USA), polyurethane (PL Premium,

Fig. 6 α as a function of dimensionless parameter $\frac{L-b}{h}$
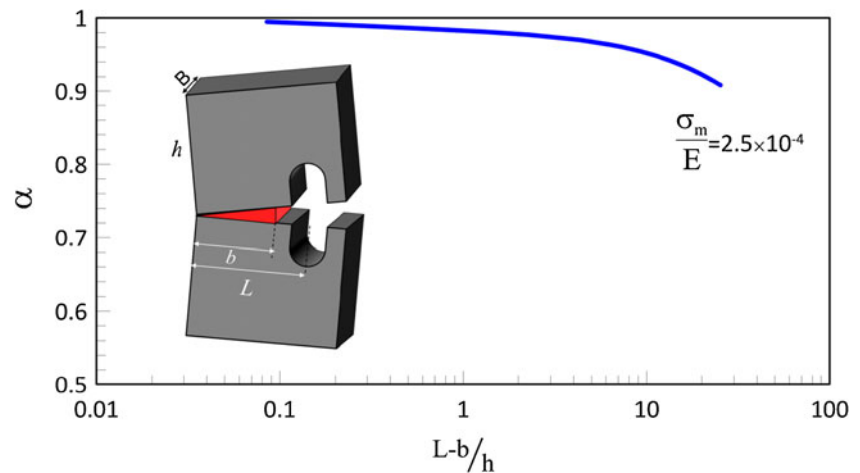
Lepage, Brampton, ON, Canada), and epoxy (EpoThin epoxy, Buehler, Lake Bluff, IL, USA). For each adhesive type a small amount of glass spheres (20 mg per 5 g of each adhesive), 30 μm in diameter (Polysciences Inc., Warrington, PA), were mixed with the glue in order to control the bond line thickness, thus minimizing any variability of toughness due to thickness variations [29]. Typical load-deflection curves resulting from RDCB tests on each of these three adhesives are shown in Fig. 7(a), while typical fracture surfaces are shown in Fig. 7(b). Polyurethane and epoxy showed essentially the same behavior: an almost linear increase at the initial part of the loading which is followed by an abrupt drop corresponding to the onset of crack propagation. In silicone the failure was more progressive, with a bell shape force-opening curve. The fracture surfaces of epoxy and silicone clearly indicated adhesive failure (the crack propagated at the adhesive-substrate interface) along one interface. Polyurethane displays a mixed failure mode including cohesive failure (the crack propagated through the adhesive), adhesive failure and crack deflections. From a fracture mechanics perspective, the latter failure mode is more desirable because it involves more energy dissipation, which translates into increased fracture toughness for the interface.

The force-deflection data obtained on epoxy, polyurethane and silicone was processed through the RDCB analysis, and Fig. 8 shows typical cohesive laws obtained for these adhesives. This data was used to measure the cohesive strength of the adhesive (maximum traction) and the maximum separation (opening at which the cohesive law vanishes). These parameters are reported in Fig. 9(a). As expected epoxy was the strongest but also the most brittle of the three adhesives, with a cohesive strength of 8-10 MPa and maximum opening of about 25 μm. In contrast, silicone showed a low cohesive strength about 10 times lower (1 MPa) but a maximum separation about 10 times larger than epoxy (200-250 um, due to the formation of ligaments across the crack faces). As a result the toughness, in energy terms, is similar for these two adhesives ($60-80$ J/m^2, Fig. 9(b)). The toughness was determined by simply measuring the area under the cohesive law. Among

all the tested adhesives, polyurethane is the toughest with average fracture toughness being approximately 430 J/m^2. This was predictable from parameters (cohesive strength and maximum separation) shown in Fig. 9(a), because it exhibits both high strength and large extensibility. Epoxy and silicone (despite being either strong or deformable) display low fracture toughness mainly due to the shortage of extensibility (in epoxy) and strength (in silicone). For impact situations where mechanical energy must be absorbed or transmitted through the adhesive without failure, epoxy and silicone therefore offer similar performances. The results we obtained here are consistent with values reported in the literature [14, 24, 30–34], although there is a considerable variation in the reported results which mainly stems from (i) surface quality of the adherends, (ii) thickness of the bondline which has a pronounced impact on the cohesive energy and subsequently the cohesive parameters of the adhesive [29], (iii) rate at which the interface is loaded, and (iv) manufacturer of the adhesive, e.g. polyurethane is manufactured with a wide range of strength in different companies. In [30], the cohesive law of toughened epoxy-steel joints is characterized by $\sigma_m=14 MPa$, $\delta_{max}=100 \mu m$, and $J_{IC}=700$ J/m^2, while the values we obtained in this study for epoxy-steel joints are $\sigma_m=9 MPa$, $\delta_{max}=30 \mu m$, and $J_{IC}=70$ J/m^2. In [30], a bond line thickness of $200 \mu m$ is reported while here the thickness of the adhesive layer was 7 times smaller resulting lower energy dissipation within the adhesive and consequently lower fracture toughness of the interface [29]. In addition here we mirror polished the surface of the steel substrates which causes lower adhesion between the adhesive and substrate (as adhesives bind more strongly to rougher substrates), and gives rise to a smaller maximum separation. A toughness of 117 J/m^2 for epoxy-aluminum joints is also reported in [35]. Sorenson et al. [14] have reported a fracture toughness of 500 J/m^2 for polyurethane-steel joints which is very close to the value we obtained in this work. For silicone adhesives, Banea et al. [36] have measured the toughness of a 1-mm thick room temperature vulcanizing (RTV) silicone adhesive (which has
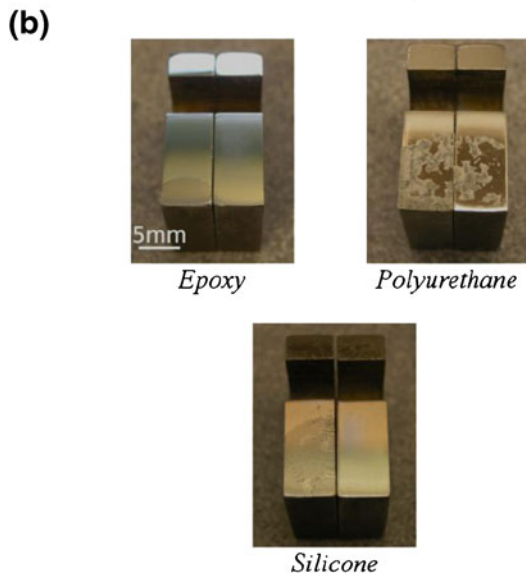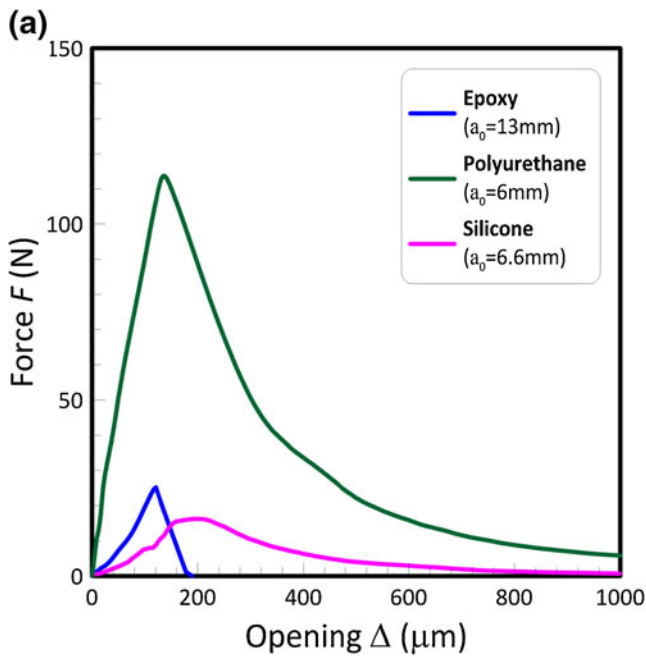
Fig. 8 Typical cohesive laws obtained from RDCB model

Fig. 7 (a) Typical force-opening curves of the three tested types of adhesive; (b) corresponding typical fracture surfaces

different composition than the adhesive tested in this work) on steel substrates. The reported value for the toughness is 2,500 J/m^2 which is significantly higher than the value we obtained here (100 J/m^2).

We finally determined the ratio α for each case in order to investigate weather the RDCB technique is valid for the selected adhesives. The position of each adhesive on the α chart is shown on Fig. 10 (epoxy: $\frac{\sigma_m}{E} = 4.6 \times 10^{-5}$ and $\frac{L-b}{h} = 0.66$, polyurethane: $\frac{\sigma_m}{E} = 2.8 \times 10^{-5}$ and $\frac{L-b}{h} = 0.30$, and silicone: $\frac{\sigma_m}{E} = 4.5 \times 10^{-6}$ and $\frac{L-b}{h} = 0.33$). For all cases, parameter α is approximately unit (maximum deviation from unit happens in the case of epoxy adhesive which is
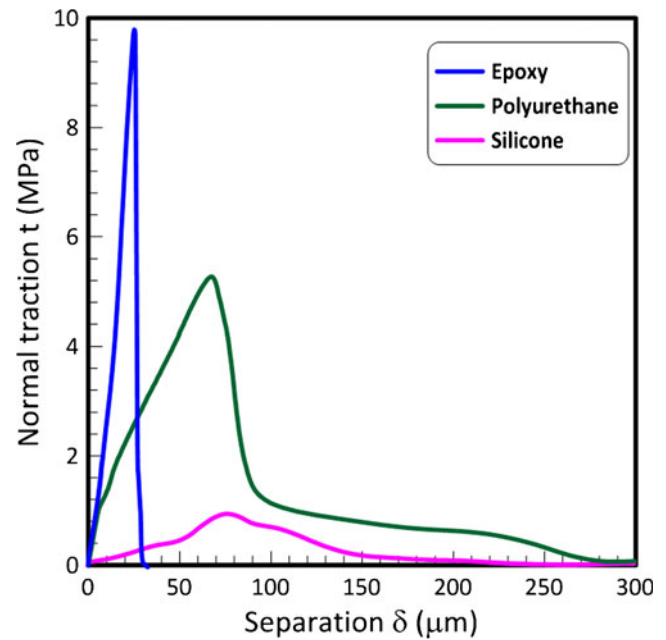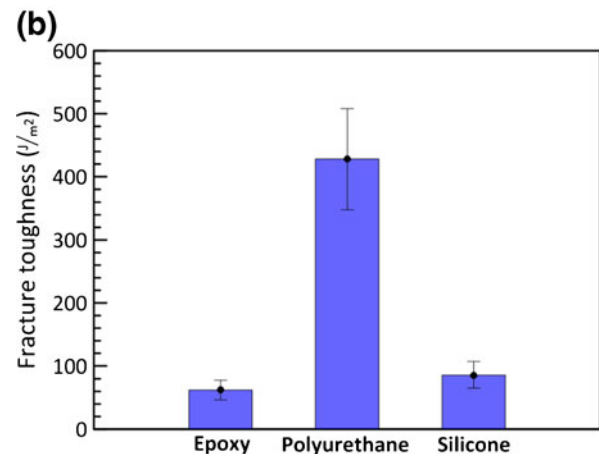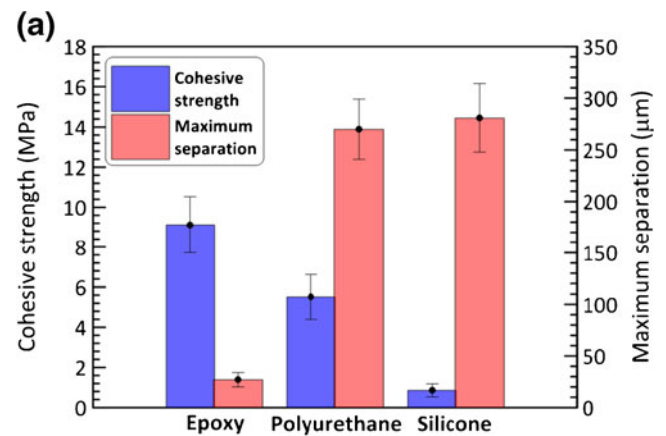

Fig. 9 Cohesive parameters for the three adhesive tested in this work: (a) cohesive strength and maximum separation, and (b) toughness
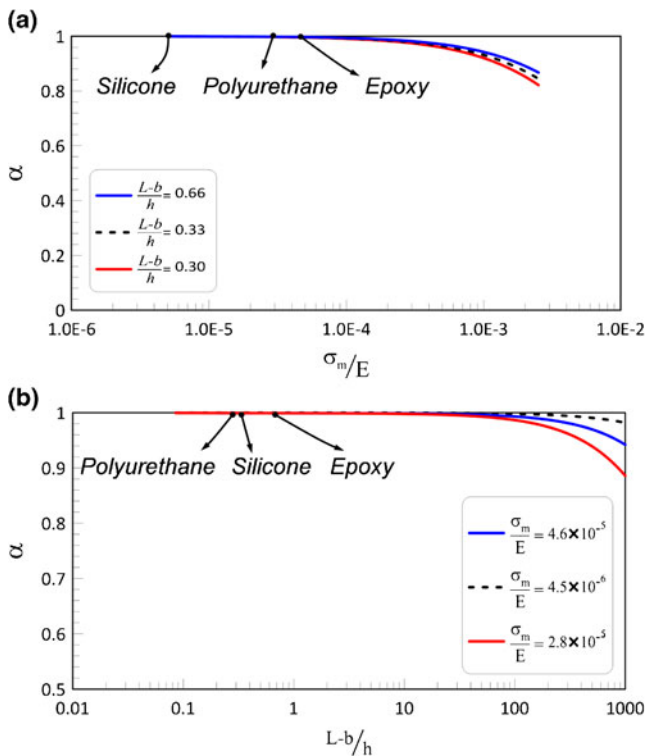
Fig. 10 Position of the tested adhesives on α chart showing that the rigidity assumption considered in the RDCB model is valid for these cases

0.3 %) which confirms that all the results presented in this study are valid and can be used for further studies on the fracture behavior of the adhesives.

Conclusions

In this article, we presented a simple experimental technique called RDCB test to determine the cohesive law and fracture toughness of engineering adhesives in mode I fracture. The RDCB method was originally developed for soft and weak biological adhesives, but we showed that the test can be modified to include high strength of engineering adhesives using thick rigid substrates. The key advantage of this method over other techniques is that it directly provides the full cohesive law of the adhesive without any initial assumption on its shape, and with no need for complex experimental setup, imaging or numerical modeling. Load-displacement data from experiment and geometry of the specimen are the only input of the RDCB model and the analysis is extremely simple. We also defined a non-dimensional parameter α which can be used to quantitatively investigate whether the assumption of rigid substrates is valid. For values of α close to unity, the RDCB rigidity assumption is valid and the method directly yields the cohesive law of the adhesive. The RDCB test was performed on three typical engineering adhesives namely polyurethane, silicone, and epoxy bonded to mirror polished steel substrates. The results showed very different cohesive laws for these adhesives. Epoxy showed high cohesive strength but small extensibility, while silicone showed high extensibility but low strength. Polyurethane, with both high strength and extensibility, was found to be the toughest of the adhesives tested here. The fracture surface of the specimens showed that a combination of adhesive and cohesive failure was dominant in the case of polyurethane which is more desirable because it involves more energy dissipation and ultimately translates into increased fracture toughness of the adhesive interface. This type of hybrid failure mode was lacking for the two other adhesives which could explain why they offer lower interfacial fracture toughness. The RDCB method is a simple yet robust and accurate method to obtain the cohesive law of adhesives, and can serve as an experimental platform to investigate their mode of failure or to optimize their performance.

References

1. Adams R, Comyn J, Wake W (1997) Structural adhesive joints in engineering. Chapman and Hall, London
2. Dunn DJ (2004) Engineering and structural adhesives. Rapra Rev Rep 15(1):1–28
3. ASTM (1986) ASTM D 3983: standard test method for measuring strength and shear modulus of nonrigid adhesives by the thick-adherend tensile-lap specimen. West Conshohocken, PA
4. Ripling EJ, Mostovoy S, Corten HT (1971) Fracture mechanics: a tool for evaluating structural adhesives. J Adhes 3(2):107–123
5. Dastjerdi AK, Pagano M, Kaartinen MT, McKee MD, Barthelat F (2012) Cohesive behavior of soft biological adhesives: experiments and modeling. Acta Biomater 8(9):3349–3359. doi:10.1016/j.actbio.2012.05.005
6. Dannenberg H (1961) Measurement of adhesion by a blister method. J Appl Polym Sci 5(14):125–134. doi:10.1002/app.1961.070051401
7. Chicot D, Démarécaux P, Lesage J (1996) Apparent interface toughness of substrate and coating couples from indentation tests. Thin Solid Films 283(1-2):151–157. doi:10.1016/0040-6090(96)08763-9
8. Lawn BR (1993) Fracture of brittle solids. Cambridge University Press, Cambridge, United Kingdom
9. ASTM (2012) ASTM D3433 - 99: standard test method for fracture strength in cleavage of adhesives in bonded metal joints. West Conshohocken, PA
10. Anderson TL (1995) Fracture mechanics: fundamentals and applications. CRC Press, Boca Raton, FL
11. Andersson T (2006) On the effective constitutive properties of a thin adhesive layer loaded in peel. Int J Fract 141(1–2):227
12. de Moura M (2012) A straightforward method to obtain the cohesive laws of bonded joints under mode I loading. Int J Adhes Adhes 39:54
13. Biel A (2010) Damage and plasticity in adhesive layer: an experimental study. Int J Fract 165(1):93
14. Sørensen BF (2003) Determination of cohesive laws by the J integral approach. Eng Fract Mech 70(14):1841

15. Carlberger T, Stigh U (2010) Influence of layer thickness on cohesive properties of an epoxy-based adhesive—an experimental study. J Adhes 86(8):816–835

16. Zhu Y, Liechti KM, Ravi-Chandar K (2009) Direct extraction of rate-dependent traction-separation laws for polyurea/steel interfaces. Int J Solids Struct 46(1):31–51

17. Shet C, Chandra N (2002) Analysis of energy balance when using cohesive zone models to simulate fracture processes. J Eng Mater Technol Trans ASME 124(4):440–450. doi:10.1115/1.1494093

18. Bouvard JL, Chaboche JL, Feyel F, Gallerneau F (2009) A cohesive zone model for fatigue and creep–fatigue crack growth in single crystal superalloys. Int J Fatigue 31(5):868–879. doi:10.1016/j.ijfatigue.2008.11.002

19. Aymerich F, Dore F, Priolo P (2009) Simulation of multiple delaminations in impacted cross-ply laminates using a finite element model based on cohesive interface elements. Compos Sci Technol 69(11–12):1699–1709. doi:10.1016/j.compscitech.2008.10.025

20. Hutchinson JW, Evans AG (2000) Mechanics of materials: top-down approaches to fracture. Acta Mater 48(1):125–135. doi:10.1016/s1359-6454(99)00291-8

21. Barthelat F, Tang H, Zavattieri PD, Li CM, Espinosa HD (2007) On the mechanics of mother-of-pearl: a key feature in the material hierarchical structure. J Mech Phys Solids 55(2):306–337. doi:10.1016/j.jmps.2006.07.007

22. Sørensen BF (2002) Cohesive law and notch sensitivity of adhesive joints. Acta Mater 50(5):1053

23. Andersson T (2004) The stress–elongation relation for an adhesive layer loaded in peel using equilibrium of energetic forces. Int J Solids Struct 41(2):413

24. Han J, Siegmund T (2012) Cohesive zone model characterization of the adhesive hysol EA-9394. J Adhes Sci Technol 26(8–9):1033–1052

25. de Moura MFSF, Morais JJL, Dourado N (2008) A new data reduction scheme for mode I wood fracture characterization using the double cantilever beam test. Eng Fract Mech 75(13):3852

26. Sun C, Thouless MD, Waas AM, Schroeder JA, Zavattieri PD (2008) Ductile–brittle transitions in the fracture of plastically-deforming, adhesively-bonded structures. Part I: Experimental studies. Int J Solids Struct 45(10):3059–3073. doi:10.1016/j.ijsolstr.2008.01.011

27. Sun C, Thouless MD, Waas AM, Schroeder JA, Zavattieri PD (2008) Ductile–brittle transitions in the fracture of plastically deforming, adhesively bonded structures. Part II: Numerical studies. Int J Solids Struct 45(17):4725–4738. doi:10.1016/j.ijsolstr.2008.04.007

28. Timoshenko S (1940) Strength of materials. Part 1: Elementary theory and problems, 2nd edn. D. Van Nostrand Company Inc., New York

29. Tvergaard V, Hutchinson JW (1994) Toughness of an interface along a thin ductile layer joining elastic solids. Philos Mag A 70(4):641–656

30. Högberg JL, Sørensen BF, Stigh U (2007) Constitutive behaviour of mixed mode loaded adhesive layer. Int J Solids Struct 44(25–26):8335–8354. doi:10.1016/j.ijsolstr.2007.06.014

31. Marzi S, Hesebeck O, Brede M, Kleiner F (2009) A rate-dependent cohesive zone model for adhesively bonded joints loaded in mode I. J Adhes Sci Technol 23(6):881–898. doi:10.1163/156856109x411238

32. Khoramishad H, Crocombe AD, Katnam KB, Ashcroft IA (2010) Predicting fatigue damage in adhesively bonded joints using a cohesive zone model. Int J Fatigue 32(7):1146–1158. doi:10.1016/j.ijfatigue.2009.12.013

33. Xu C, Siegmund T, Ramani K (2003) Rate-dependent crack growth in adhesives II. Experiments and analysis. Int J Adhes Adhes 23(1):15–22. doi:10.1016/S0143-7496(02)00063-5

34. Zhu Y, Liechti KM, Ravi-Chandar K (2009) Direct extraction of rate-dependent traction–separation laws for polyurea/steel interfaces. Int J Solids Struct 46(1):31–51. doi:10.1016/j.ijsolstr.2008.08.019

35. Meng Q, Zaman I, Hannam JR, Kapota S, Luong L, Youssf O, Ma J (2011) Improvement of adhesive toughness measurement. Polym Test 30(2):243–250. doi:10.1016/j.polymertesting.2011.01.001

36. Banea MD, da Silva LFM, Campilho RDSG (2010) Temperature dependence of the fracture toughness of adhesively bonded joints. J Adhes Sci Technol 24(11–12):2011–2026. doi:10.1163/016942410x507713